在HIAF&PKMu上寻找CLFV过程 $\mu^+e^- \rightarrow \phi$

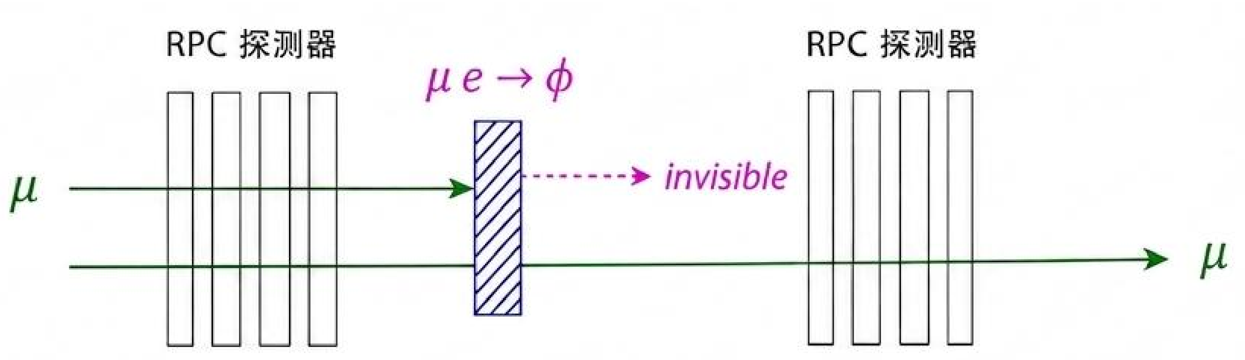

报告人：沈锦鸿
7月12日 北京大学

合作者：**沈锦鸿**、吴友鹏、王子健、高乐耘等

目录

- 简介：带电轻子味道破坏 (Charged Lepton Flavour Violation)
- 理论：$\mu^+ e^- \rightarrow \phi$
- 数值结果和模拟
- HIAF&PKMu装置和预期实验

带电轻子味道破坏

- 轻子味道破坏 (Lepton Flavour Violation) 指破坏独立轻子数 (L_e, L_μ, L_τ) 守恒的物理过程

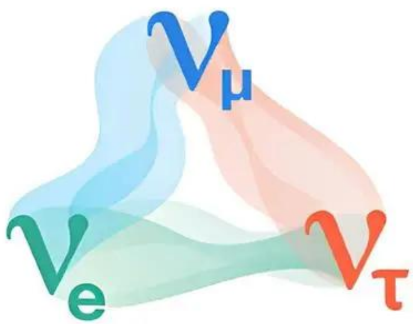

中性轻子味道破坏
Neutral LFV (NLFV)

由中微子质量振荡解释

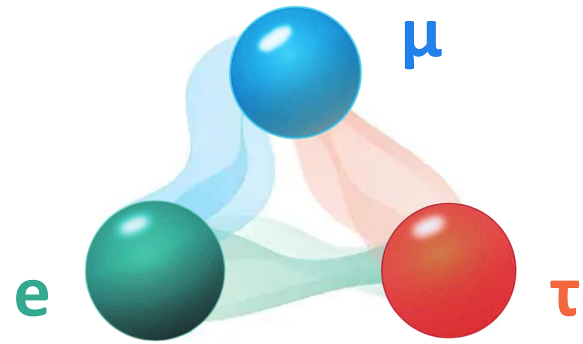

带电轻子味道破坏
Charged LFV (CLFV)

标准模型框架内产率极小 ($\mu \to e\gamma$ Br～ 10^{-54})
[Frau & Langenbruch, 2024]

★ 任何实验上的观测将直接指向新物理！

已有/预期CLFV实验结果

https://indico.ihep.ac.cn/event/21331/contributions/160792/

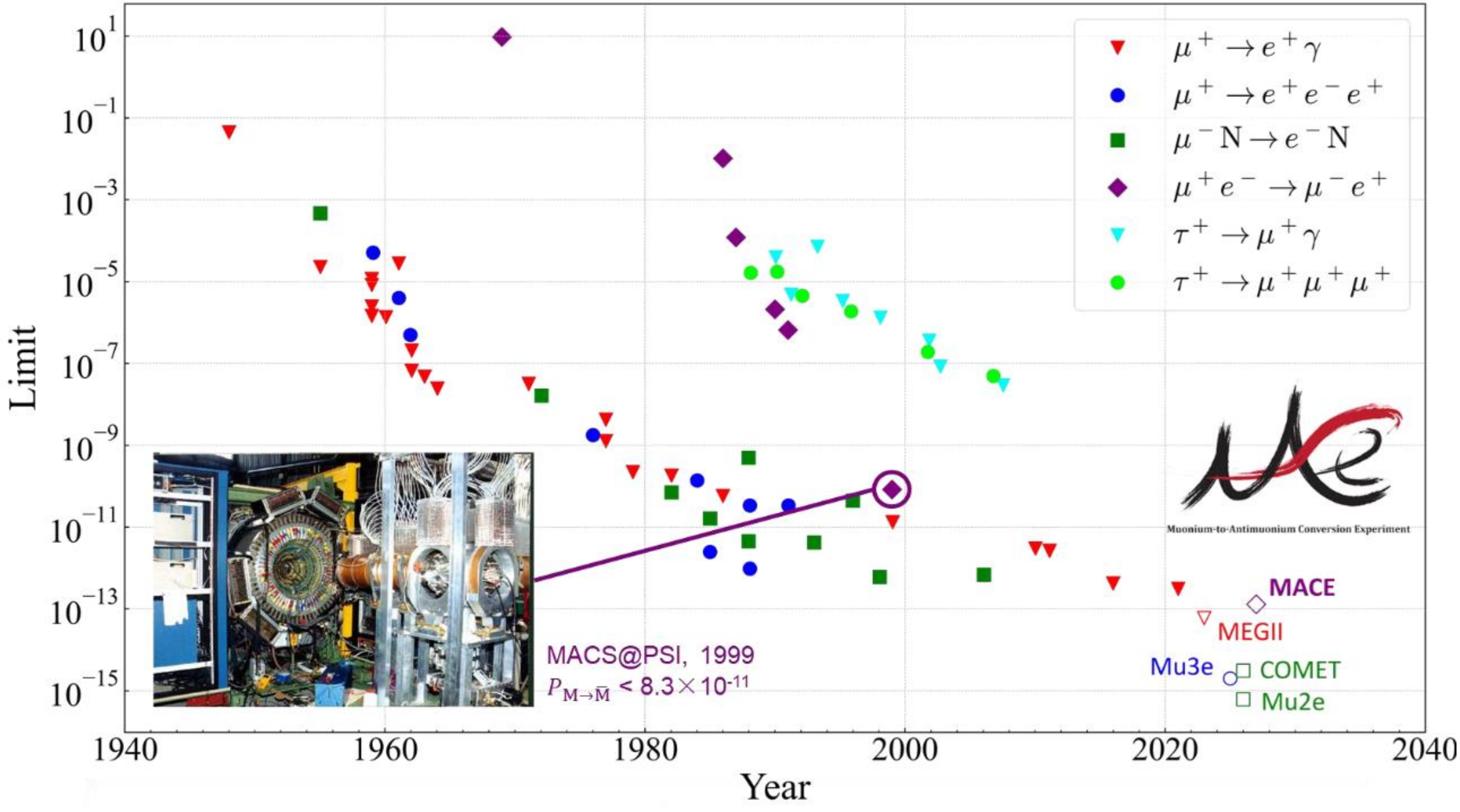

$\mu^+ e^- \rightarrow \phi$

$$\mathcal{L}_{\rm int} = -\phi\left(y_{e\mu}\, \overline{e}\, \mu + y_{\mu e}\, \overline{\mu}\, e\right) + {\rm h.c.}$$

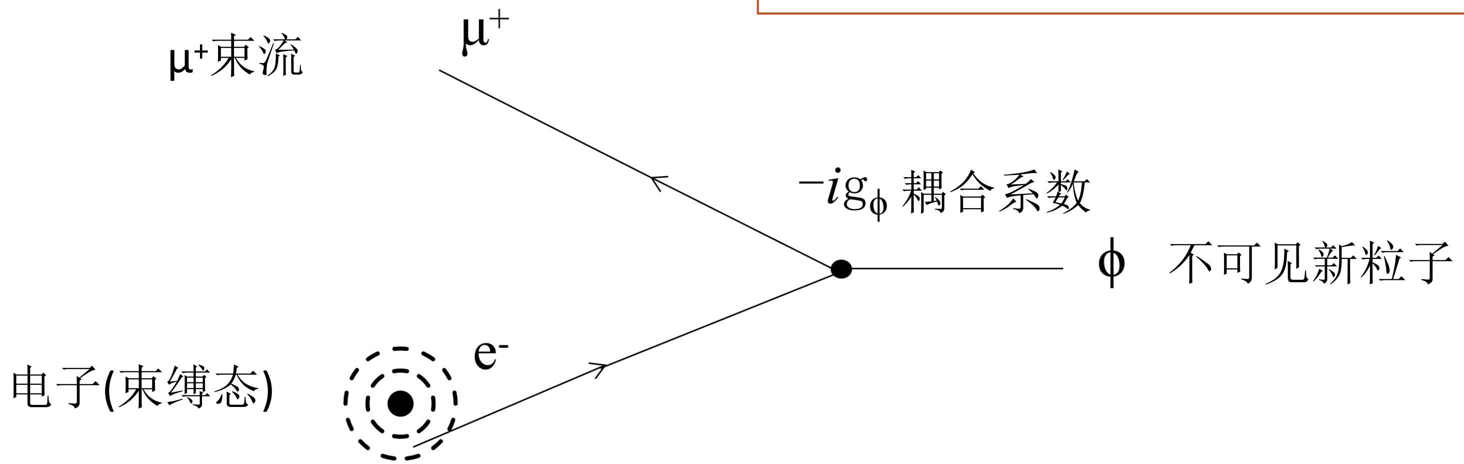

- 通常的高能物理计算假设电子自由且静止。但对于湮灭过程，共振质量附近电子的**动量分布会显著影响反应截面，**我们采用**束缚态狄拉克旋量**处理靶电子:

电子动量

$$\mathcal{U}_{E\kappa m} = \frac{4\pi}{k_A}(-i)^l \begin{bmatrix} g_{E\kappa}\, \mathcal{Y}_{+\kappa m}\left(\hat{\mathbf{k}}_{\mathbf{A}}\right) \\ -f_{E\kappa}\, \mathcal{Y}_{-\kappa m}\left(\hat{\mathbf{k}}_{\mathbf{A}}\right) \end{bmatrix}$$

归一化

$$\frac{1}{(2\pi)^3} \sum_m \int \mathcal{U}^\dagger_{E\kappa m} \mathcal{U}_{E\kappa m}\, d^3 k_A = 2E_A$$

径向分量：f,g函数，由Roothan-Hartree-Fock (RHF) 程序数值解出

角向分量：旋量球谐函数

$\mu^+ e^- \to \phi$

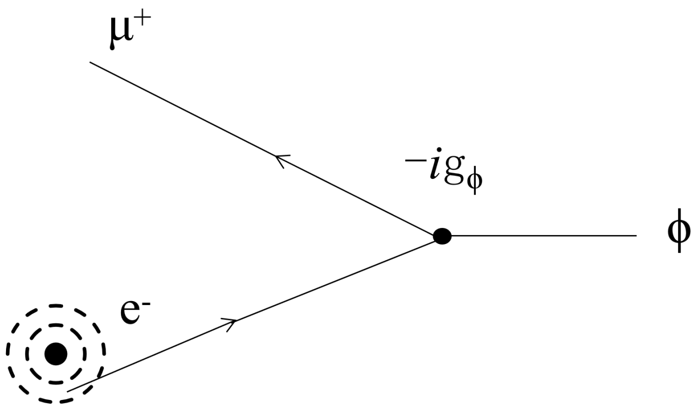

散射振幅平方和反应截面计算

$$\sigma = \sum_Z \sigma_{E\kappa} = \sum_Z \int \frac{d^3 k_A}{(2\pi)^3} \frac{|\mathcal{M}|^2_\kappa}{2E_B |v_B|} d\Phi$$

$$d\Phi = (2\pi)^4 \delta(E_A + E_B - E_\phi)\delta^{(3)}(\mathbf{k_A} + \mathbf{p_B} - \mathbf{p_\phi}) \frac{d^3 p_\phi}{(2\pi)^3 2E_\phi}.$$

结果

束缚态振幅平方

$$\overline{|\mathcal{M}|^2_\kappa} = \frac{2(2j+1)\pi g_\phi^2}{k_A^2}\left[g^2(E_B - m_B) - 2gf\left(\mathbf{p_B}\cdot\hat{\mathbf{k}}_\mathbf{A}\right) + f^2(E_B + m_B)\right]$$

静止自由电子振幅平方

$$|\mathcal{M}|^2 = 2g_\phi^2(E_A E_B - m_A m_B)$$

数值计算反应截面

$$\sigma = \sum_Z \int_{k_A^{min}}^{k_A^{max}} \frac{(2j+1)g_\phi^2[(E_B - m_B)g^2 - 2gfp_B x_0 + f^2(E_B + m_B)]}{8p_B^2 E_A k_A} dk_A$$

和理论物理学家们的合作

- 本工作得到 **Luc Darmé** (法国里昂大学) 和 **Huasheng Shao** (LPTHE) 两位理论物理学家的支持。他们长期从事轻暗物质、束缚电子效应、高能过程软件模拟等研究。

- 前期工作中，他们采用 Compton Profile (CP) 和 Roothan-Hartree-Fock (RHF) 方法研究了 PADME 实验中 $e^+e^- \to X_{17}$ 过程的束缚态电子修正效应。我们与他们合作开展基于 Dirac 旋量 f,g 分量的更高精度的计算，并采用其提供的 f,g 函数数值结果作为本工作的重要输入参数。

束缚态修正

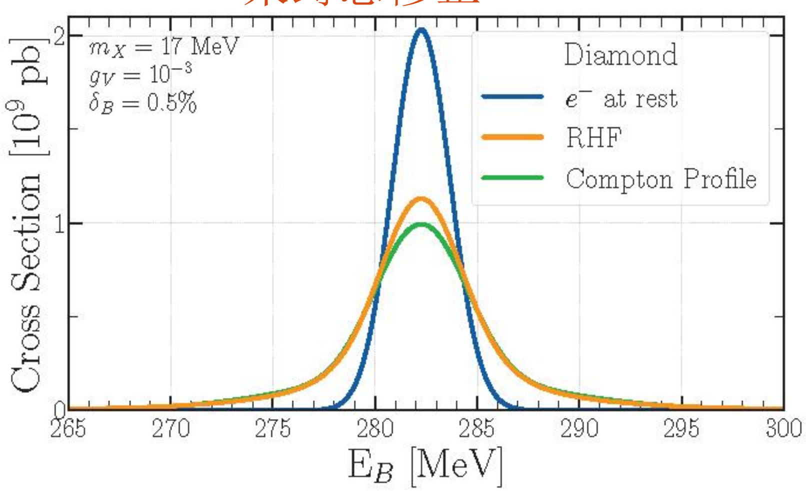

Phys. Rev. Lett. 133, 219901 (2024)

Zoom 会议

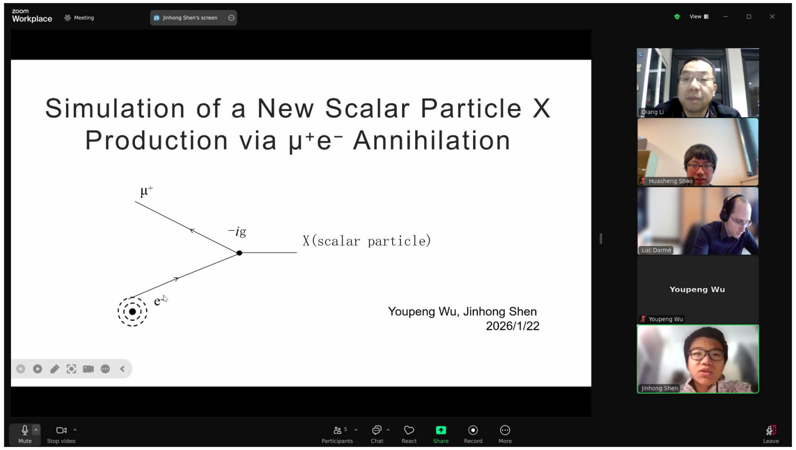

不同方法得到的散射截面对比

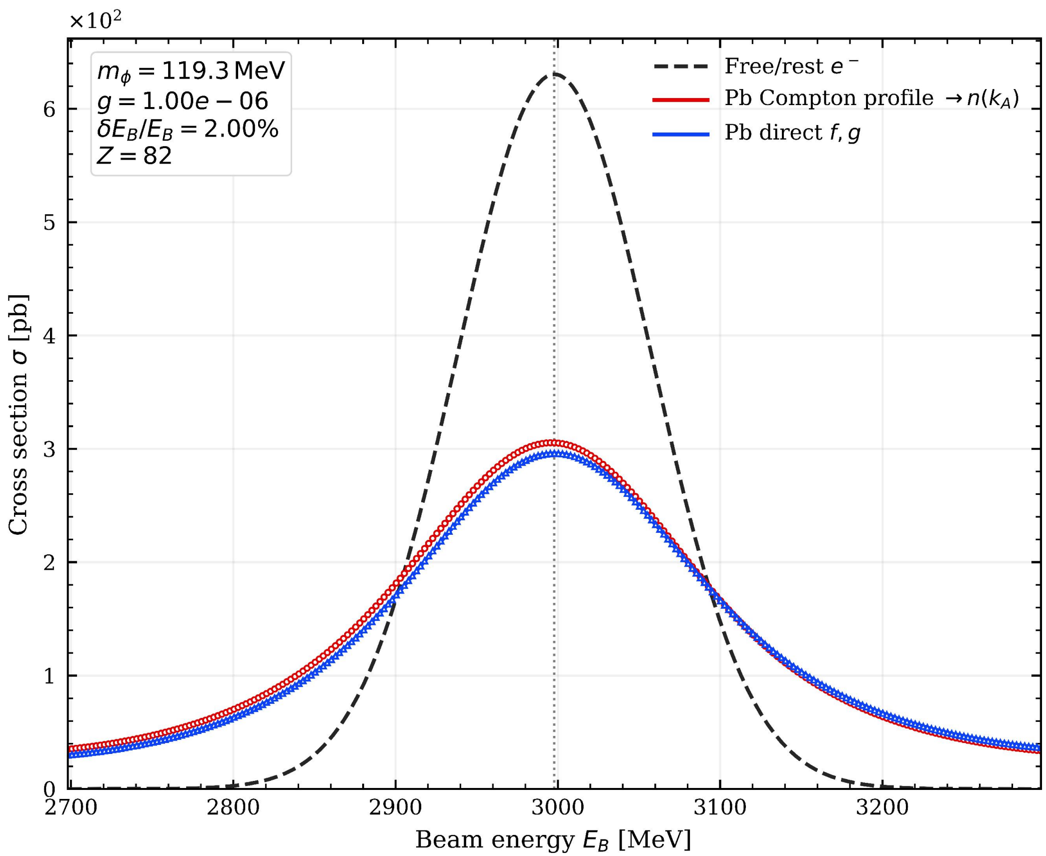

1. 静止自由电子假设 --

VS

2. Compton profile方法 —

VS

3. f,g 函数方法 —

➤ 考虑束缚态电子动量分布，修正显著!

PKMu 探测器 @ HIAF实验

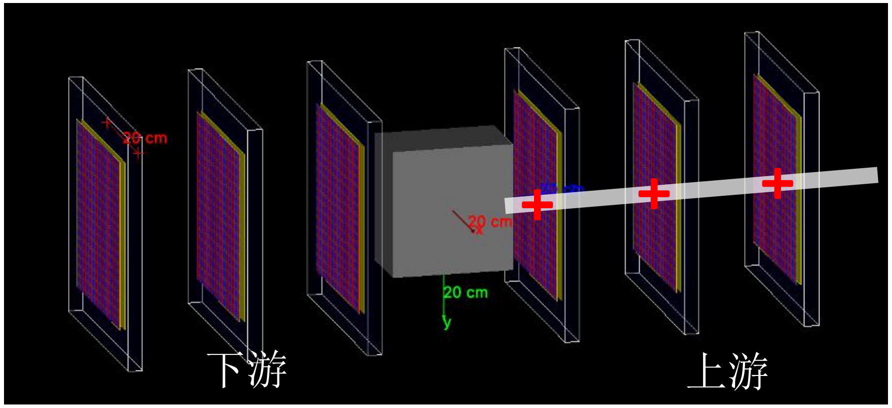

- 6 层 RPC (3 上游 & 3 下游)
- 距离: 300 mm / 170 mm
- 敏感区: 280 mm × 280 mm
- 靶材参数: 120 mm × 210 mm × 200 mm Pb

- 信号 + 89 个背景过程
- ϕ 不可见衰变

- 束流能量: 3 GeV
- 强度: 7.5×10^{5} μ^{+}/s
- 束斑尺寸: $\sigma_x = \sigma_y = 30$ mm
- 生成事例数: 2.5×10^{7}

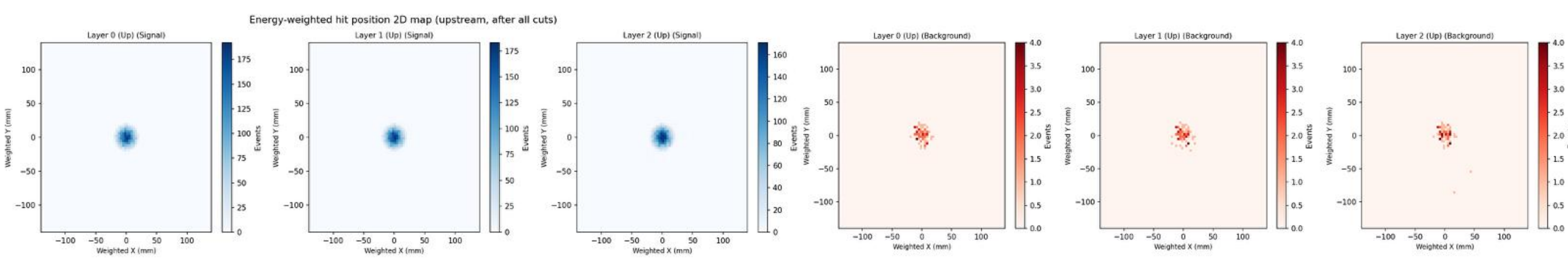

对比

- 24小时 (6.5×10^{10} MOT) 就可以在共振质量附近得到目前国际最优结果。
- 后续可以通过改变束流能量对共振质量做扫描，获得更大质量范围的优势结果。

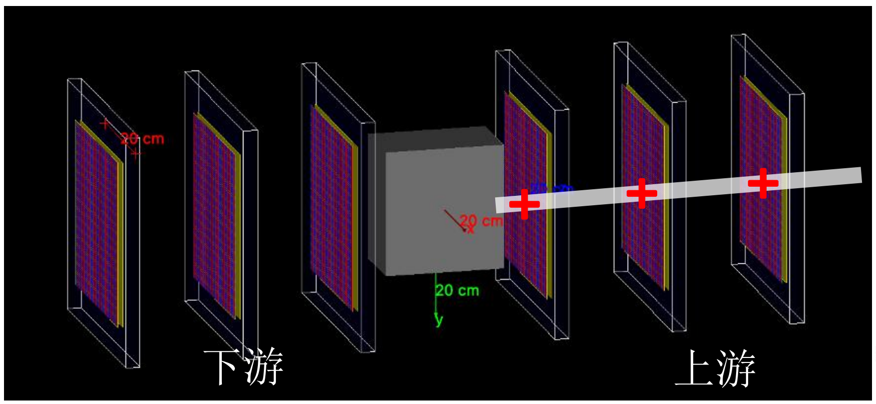

筛选 1. 上游符合
筛选 2. 下游否决
筛选 3. 束斑半径 r0<30mm
筛选 4. 靶点指向

≈ 20.7%

Table 1. Cutflow summary for signal and background events.

Process	Generated	Cut 1	Cut 2	Cut 3	Cut 4
Signal	221,983	221,983	219,061	46,108	45,969
Background	24,769,782	24,764,801	2,211	395	387

- 99.999%

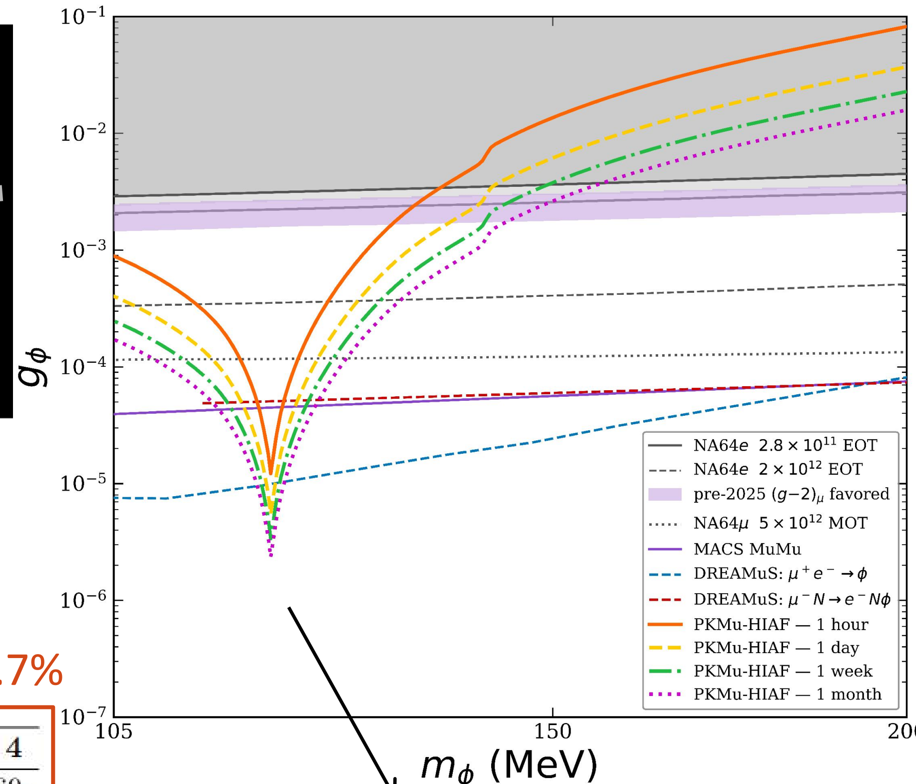

我们的结果

HIAF装置

广东，惠州，HIAF园区航拍图

https://www.imp.cas.cn/hiaf/

中国科学院近代物理研究所（IMP）在建的强流重离子加速器装置（HIAF）可提供 7.5×10^5 μ^+/s , 中心能量 3GeV，能量展宽 2% 缪子束流

doi:10.1103/PhysRevAccelBeams.28.053401

预期实验结果

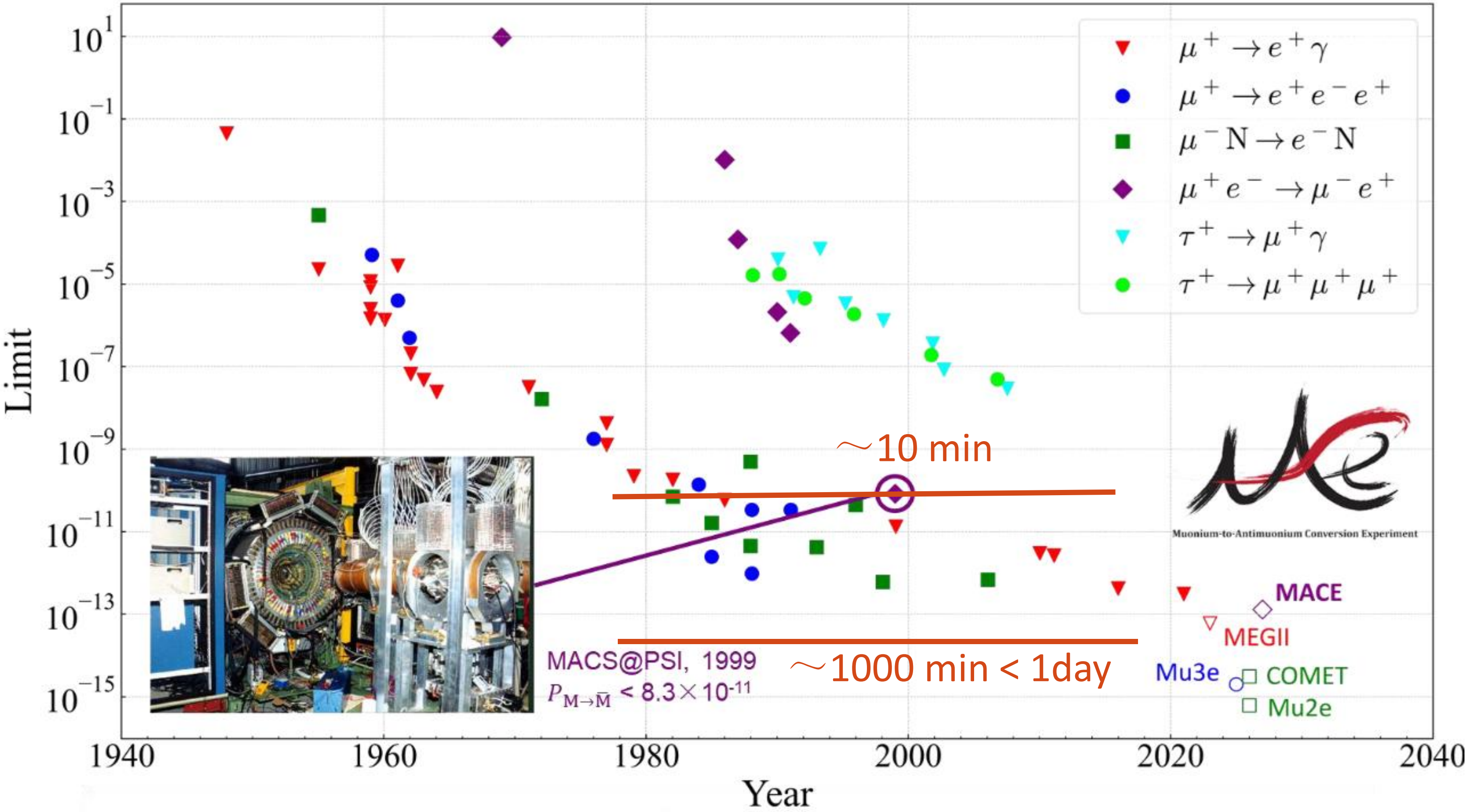
Limit
Year
$\mu^+ \to e^+ \gamma$
$\mu^+ \to e^+ e^- e^+$
$\mu^- N \to e^- N$
$\mu^+ e^- \to \mu^- e^+$
$\tau^+ \to \mu^+ \gamma$
$\tau^+ \to \mu^+ \mu^+ \mu^+$
～10 min
～1000 min < 1day
MACS@PSI, 1999
$P_{M \to \bar{M}} < 8.3 \times 10^{-11}$
Muonium-to-Antimuonium Conversion Experiment
MACE
MEGII
Mu3e
COMET
Mu2e

总结

- 我们利用束缚态电子理论体系，得到了CLFV过程 $\mu^+e^- \rightarrow \phi$ 的理论反应截面。
- 我们利用 PKMu 探测体系，对预期结果做了模拟。结论是只需 HIAF 短时间 (1 天) 束流就可以在 119MeV 质量附近取得国际最佳结果。

感谢聆听，敬请批评指正

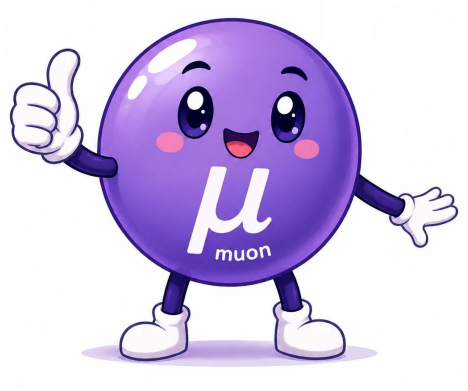

Back up

Compton profile (康普顿轮廓)

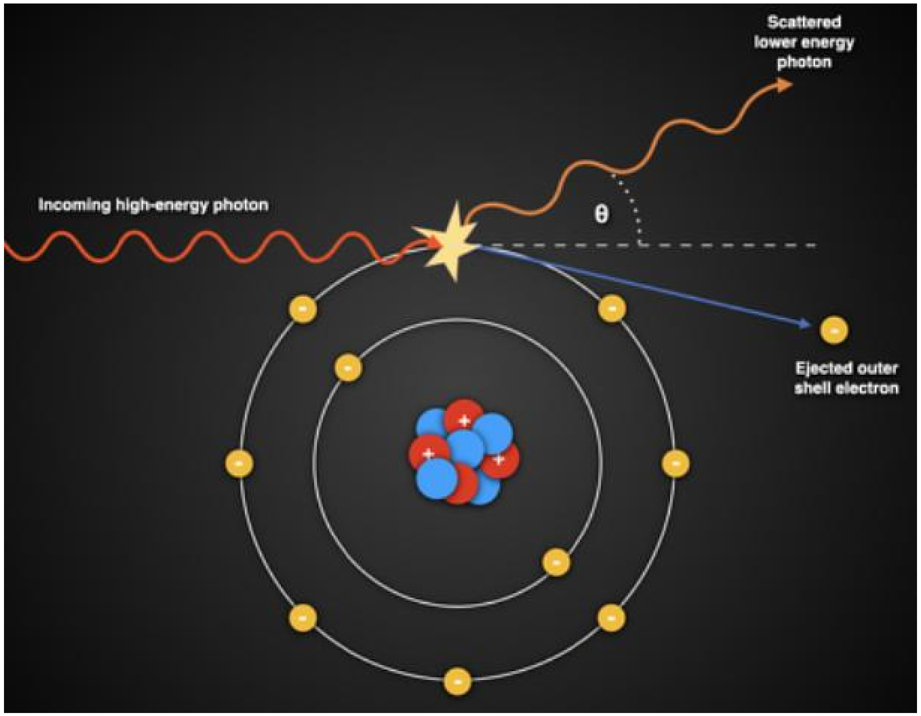

Electron momentum density.—The key input for the calculation of the resonant cross section is the electron momentum distribution $n_A(k_A)$. For most of the elements, this quantity has been extracted directly from measurements of the CP [30]. In this Letter, we focus on electron momentum density from spherically averaged Compton profiles, $J(p)$, defined as [31]

$$J(p) = \frac{1}{2}\int_{|p|}^{\infty} \rho(k) k dk, \tag{10}$$

where $\rho(k)$ is the electron momentum distribution normalized as $\int_{-\infty}^{\infty} J(p) dp = Z$, which, in our notation, can be rewritten as $\rho(k) = [n(k)/2\pi^2]$. The electron momentum density distribution and the CP are then related as

$$n(k) = -\frac{(2\pi)^2}{k}\frac{dJ(k)}{dk}. \tag{11}$$

Data source: https://www.sciencedirect.com/science/article/pii/0092640X75900303

旋量球谐函数

$$\mathcal{Y}_{\kappa m}(\hat{\mathbf{x}}) = \langle \hat{\mathbf{x}} | l_{1/2} j m \rangle; \qquad j = |\kappa| - \frac{1}{2}, \quad l = \begin{cases} \kappa, & \kappa > 0 \\ -(\kappa+1), & \kappa < 0 \end{cases} \tag{21}$$

in which l is the orbital angular momentum quantum number, j is the total angular momentum quantum number, and m is the magnetic quantum number. And for spin 1/2 systems like electrons, the explicit form of the spinor spherical harmonics is

$$\mathcal{Y}_{l,\pm\frac{1}{2},j,m} = \frac{1}{\sqrt{2(j \mp \frac{1}{2}) + 1}} \begin{bmatrix} \pm\sqrt{(j \mp \frac{1}{2}) \pm m + \frac{1}{2}}\, Y_l^{m-\frac{1}{2}} \\ \sqrt{(j \mp \frac{1}{2}) \mp m + \frac{1}{2}}\, Y_l^{m+\frac{1}{2}}. \end{bmatrix} \tag{22}$$

In momentum space, we perform a Fourier transform on the above wavefunction form to obtain the wavefunction form in momentum space:

$$\mathcal{U}_{E\kappa m}(\mathbf{p}) = \frac{4\pi}{p}(-i)^{\,l} \begin{bmatrix} g_{E\kappa}(p)\, \mathcal{Y}_{+\kappa m}(\hat{\mathbf{p}}) \\ -f_{E\kappa}(p)\, \mathcal{Y}_{-\kappa m}(\hat{\mathbf{p}}) \end{bmatrix} = \frac{4\pi}{p}(-i)^{\,l} \begin{bmatrix} g_{E\kappa}(p) \\ f_{E\kappa}(p)\,(\boldsymbol{\sigma}\cdot\hat{\mathbf{p}}) \end{bmatrix} \mathcal{Y}_{+\kappa m}(\hat{\mathbf{p}}) \tag{23}$$

f,g函数

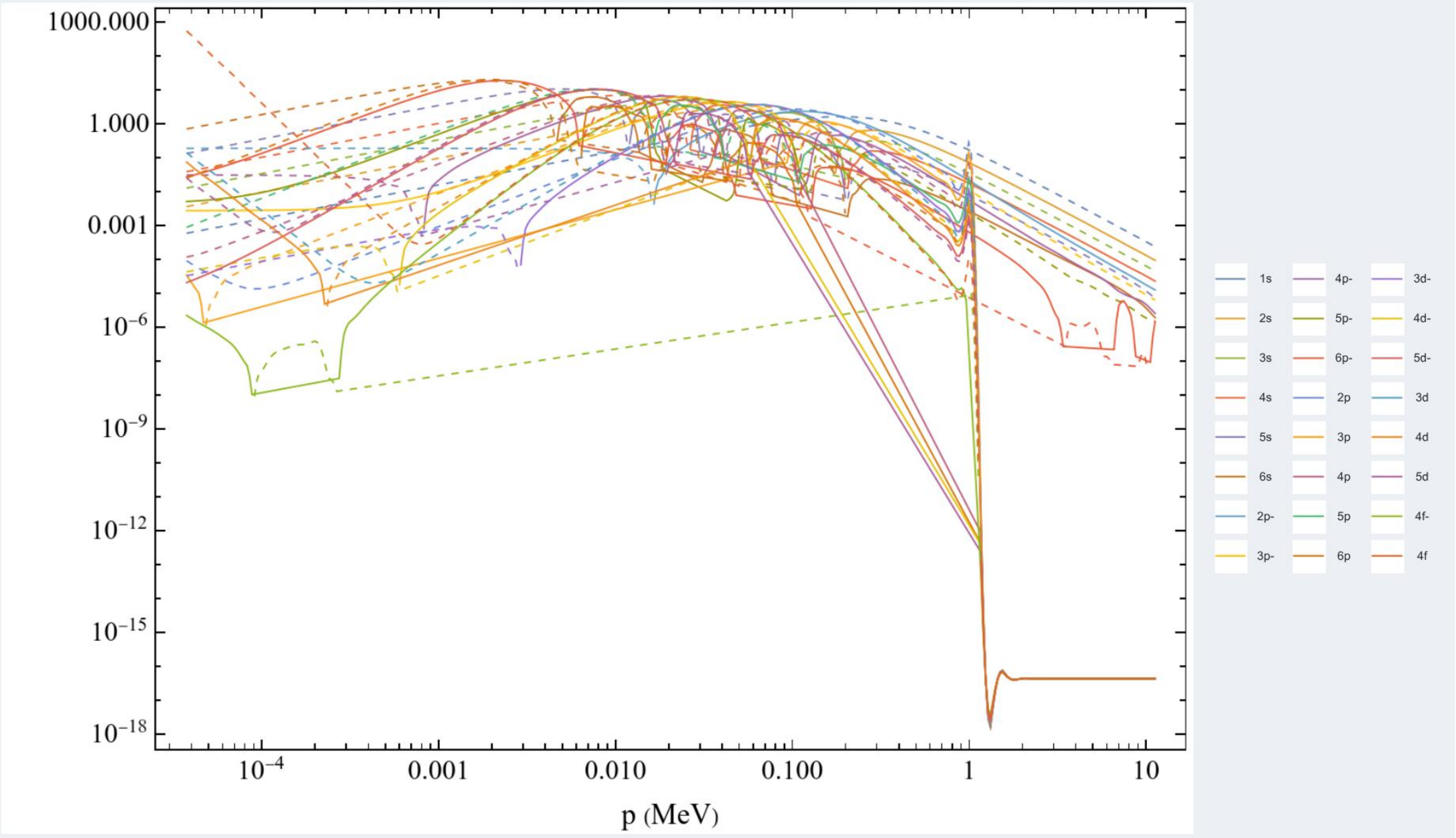
1000.000
1.000
0.001
10^{-6}
10^{-9}
10^{-12}
10^{-15}
10^{-18}
10^{-4}
0.001
0.010
0.100
1
10
p (MeV)
1s
2s
3s
4s
5s
6s
2p-
3p-
4p-
5p-
6p-
2p
3p
4p
5p
6p
3d-
4d-
5d-
3d
4d
5d
4f-
4f

交叉检验

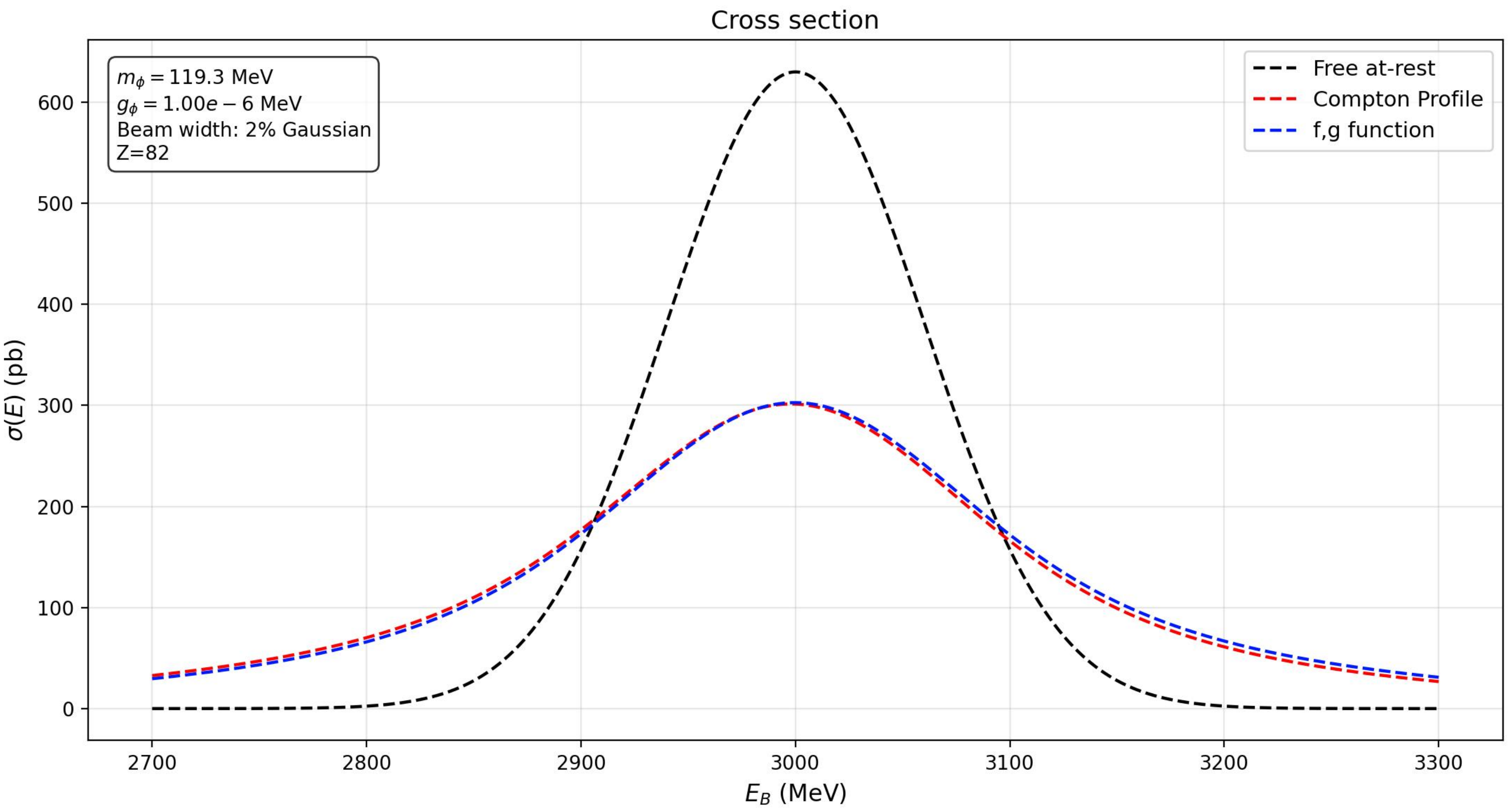
Cross section
$m_\phi = 119.3$ MeV
$g_\phi = 1.00e-6$ MeV
Beam width: 2% Gaussian
Z=82
Free at-rest
Compton Profile
f,g function
600
500
400
300
200
100
0
σ(E) (pb)
2700
2800
2900
3000
3100
3200
3300
E_B (MeV)

1%能散

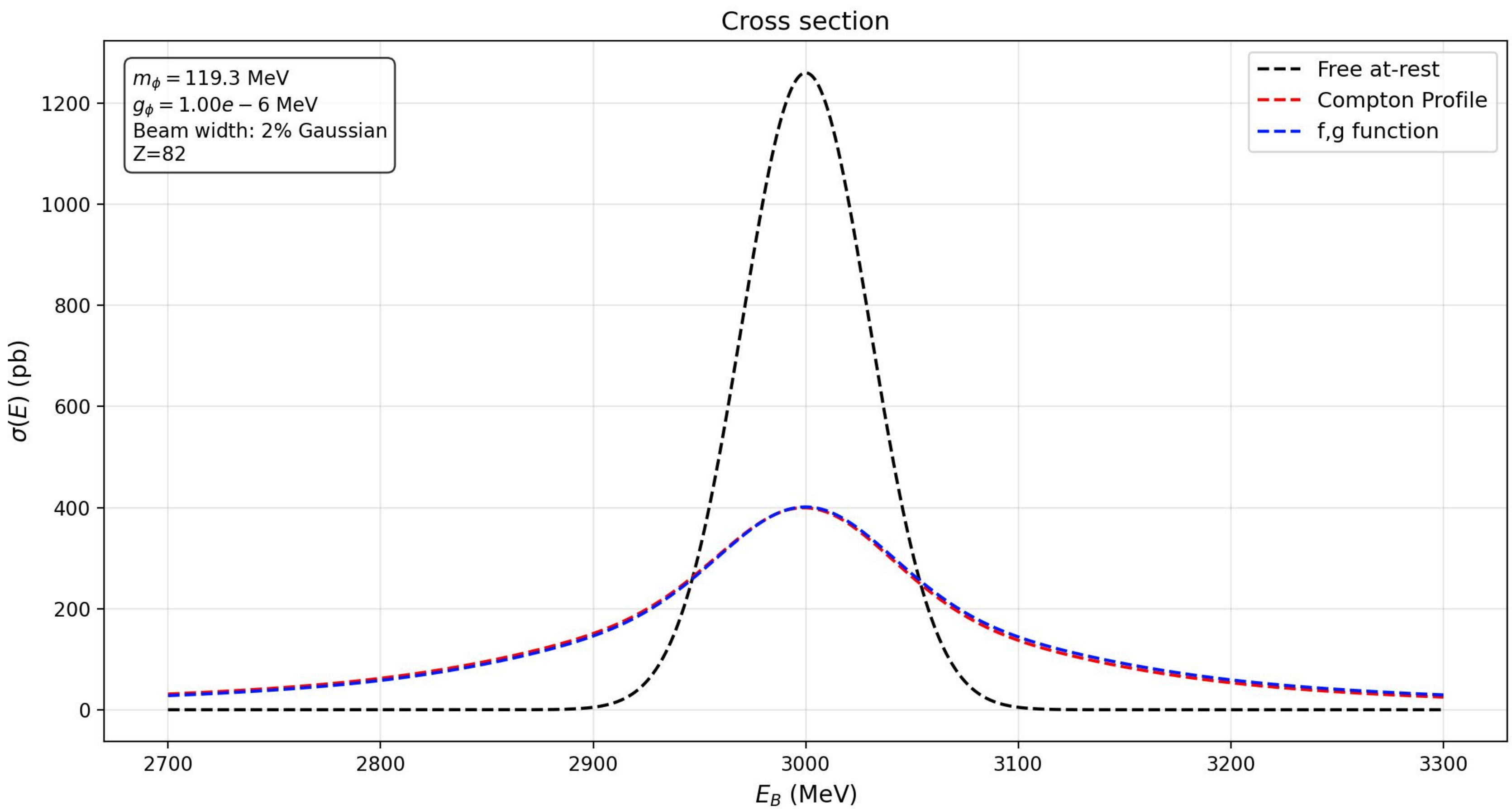
Cross section
$m_\phi = 119.3$ MeV
$g_\phi = 1.00e-6$ MeV
Beam width: 2% Gaussian
Z=82
Free at-rest
Compton Profile
f,g function
1200
1000
800
600
400
200
0
σ(E) (pb)
2700
2800
2900
3000
3100
3200
3300
E_B (MeV)

能散与运动效应对比

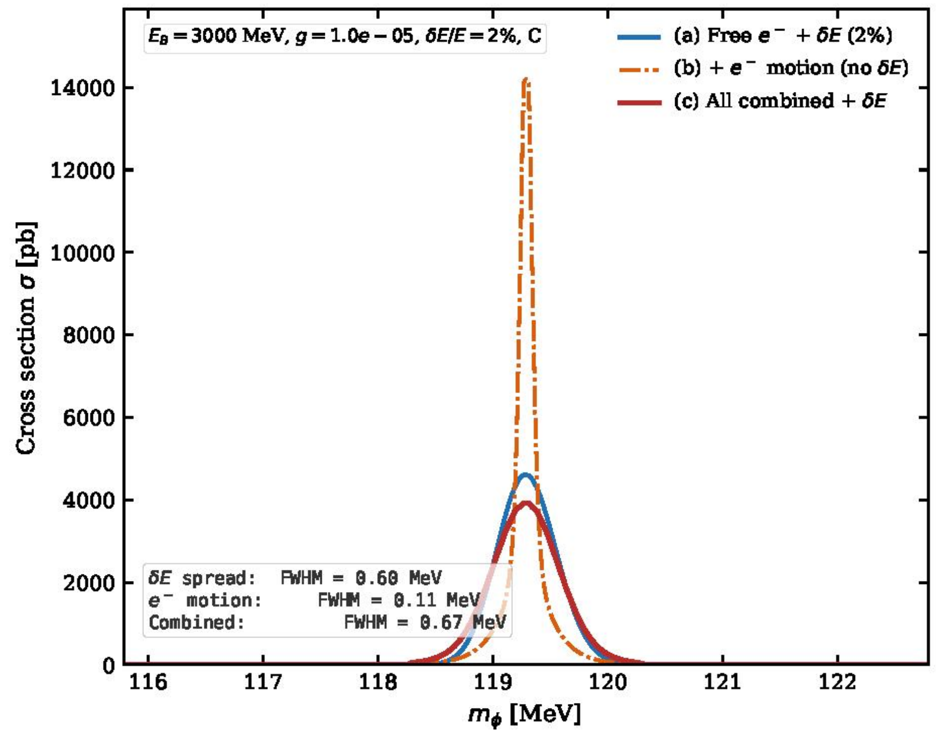

图 3: 各个效应带来的展宽: a) 只考虑束流能散 b) 只考虑束缚电子运动 c) 同时考虑两者。参数在图上标注

其他CLFV实验

1. **$\mu^+ \to e^+\gamma$**
   - MEG experiment at the Paul Scherrer Institut (PSI) in Switzerland (2009-2013)
   - 7.5×10^{14} stopped muons on target
   - $B(\mu^+ \to e^+\gamma) < 4.2 \times 10^{-13}$ (90%CL)
   - doi:10.1140/epjc/s10052-016-4271-x
2. **$\mu^+ \to e^+e^-e^+$**
   - the πE3 channel of the Swiss Institute for Nuclear Research (SIN)
   - 7.3×10^{12} μ^+ were stopped in an 11 mg/cm2 foam target.
   - $B(\mu^+ \to e^+e^-e^+) < 2.4 \times 10^{-12}$ (90%CL)
   - Six weeks were spent for the actual data taking
   - The average beam intensity during the experiment was 7×10^6 s^{-1}
   - About 93% of the beam was stopped inside the spectrometer.
   - doi:10.1016/0550-3213(85)90308-6
3. **$\mu^- \to e^-$ in nuclei**
   - μ−e conversion in muonic gold performed with the SINDRUMII spectrometer at PSI
   - $\Gamma(\mu^- Au \to e^- Au g.s.)/\Gamma_{capture}(\mu^- Au) < 7 \times 10^{-13}$ (90% C.L.)

Whereas highest experimental sensi tivities were reached in dedicated μ and K experiments, τ decay starts to become interesting as well [7–9] doi:10.1140/epjc/s2006-02582-x

MACS

$(V \pm A) \times (V \pm A)$ [20,21]. For these cases the traditionally quoted upper limit for the coupling constant is $G_{M\overline{M}} = G_F\sqrt{P_{M\overline{M}}(0\ \mathrm{T})/2.56 \times 10^{-5}} \le 3.0 \times 10^{-3} G_F$ (90% C.L.), where G_F is the Fermi coupling constant.

```
In[53]:= GF = 1.1663787 * 10^-11;
         GW = 3.0 * 10^-3 * GF;
         factor = Sqrt[2 * Sqrt[2] * GW];
                  平方根   平方根
         Plot[factor * x, {x, 106, 200}, PlotLabel → "gphi", AxesLabel → {"x", "y"}, PlotStyle → {Blue, Thick}, GridLines → Automatic,
         绘图                               绘图标签                 坐标轴标签                 绘图样式      蓝色  粗              网格线       自动
          BaseStyle → {FontSize → 12}, ScalingFunctions → {"Linear", "Log"}]
          基本样式       字体大小          刻度函数
```

Out[56]=

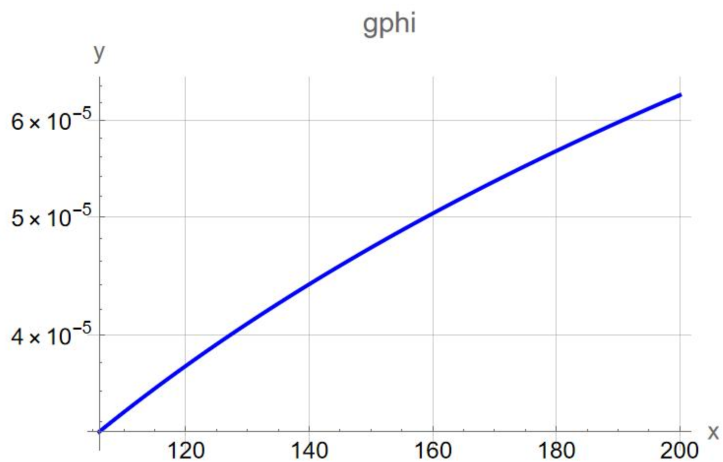

https://journals.aps.org/prl/pdf/10.1103/PhysRevLett.82.49

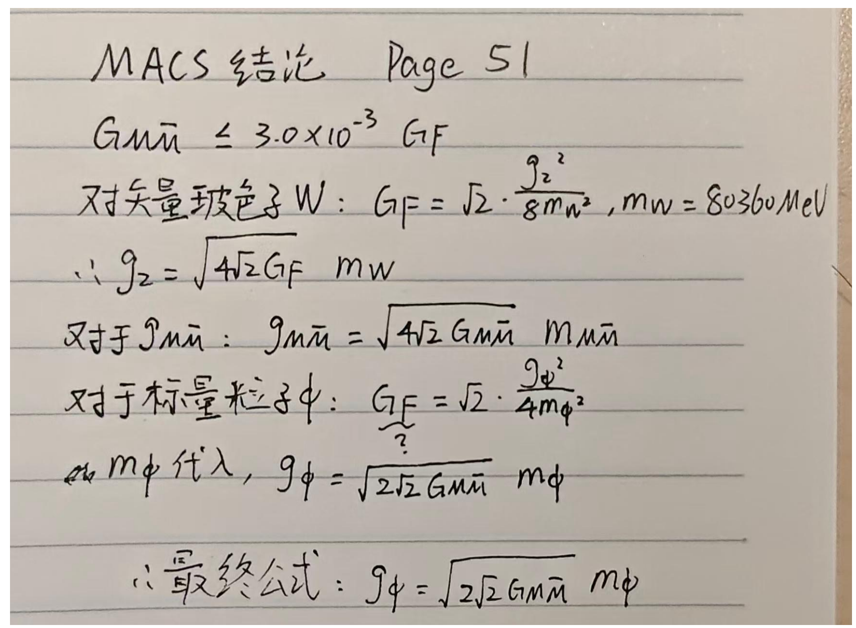

MACS 结论 Page 51

$G_{M\bar{M}} \le 3.0\times10^{-3}\, G_F$

对矢量玻色子W: $G_F=\sqrt{2}\cdot\frac{g_2^2}{8m_W^2}$, $m_W=80360\,\mathrm{MeV}$

∴ $g_2=\sqrt{4\sqrt{2}G_F}\, m_W$

对于 $g_{M\bar{M}}$: $g_{M\bar{M}}=\sqrt{4\sqrt{2}G_{M\bar{M}}}\, m_{M\bar{M}}$

对于标量粒子φ: $G_F \overset{?}{=} \sqrt{2}\cdot\frac{g_\phi^2}{4m_\phi^2}$

m_ϕ 代入, $g_\phi=\sqrt{2\sqrt{2}G_{M\bar{M}}}\, m_\phi$

∴最终公式: $g_\phi=\sqrt{2\sqrt{2}G_{M\bar{M}}}\, m_\phi$

CLFV实验

1. μ→eγ：对偶极（dipole）算符最敏感的 cLFV 通道，双体末态信号极其干净，能够直接检验圈图诱导的轻子味破坏机制。
2. μ→3e：兼具圈图与树级四轻子贡献的探针，无强子理论误差，但多粒子末态带来更高实验重建复杂度。
3. μN→eN：对半轻子（lepton–quark）相互作用最敏感的 cLFV 通道，受益于核相干增强，通常对应最高的新物理能标探测能力。
4. 缪子偶素转变：完全由轻子组成的体系，无强子结构不确定性，是检验纯轻子 LFV 相互作用和特定 $\Delta L_e=\Delta L_\mu=2$ 新物理的重要平台。
5. μe湮灭：唯一能够直接共振产生 LFV 介导粒子的 μe 过程；信号拓扑简单，对轻质量新粒子和共振增强效应尤为敏感。

HIAF

3.1 Experimental Setup

The proposed experiment is designed to run at the High Intensity heavy-ion Accelerator Facility (HIAF) [29], currently under construction at the Institute of Modern Physics (IMP) in Huizhou, China. HIAF delivers ion beams ranging from protons to uranium with energies of order GeV/u and intensities up to 10^{11}–10^{12} particles per pulse. The muon beam is produced and transported by the High energy FRagment Separator (HFRS) beamline [30], which is 192 m long with a maximum magnetic rigidity of 25 Tm, enabling the transport of muons with momenta up to 7.5 GeV/c. Using a 9.3 GeV proton primary beam incident on a graphite target, pions are produced and subsequently decay in flight along the beamline; the total HFRS length is well-matched to the decay length of a ∼3 GeV/c pion (≈ 170 m). A two-section magnetic rigidity purification strategy raises the μ^+ beam purity to 100% at an intensity of $\mathcal{O}(10^5)$ μ^+/s [30]. For the present study, we adopt the benchmark parameters $E_B = 3$ GeV, an intensity of 7.5×10^5 μ^+/s, and a transverse beam spot of $\sigma_x = \sigma_y = 30$ mm.

Crucially, the resonance condition $\sqrt{s} = m_\phi$ for $\mu^+ e^- \to \phi$ on atomic electrons at rest maps a 3 GeV muon beam onto scalar masses in the range 100–200 MeV—precisely the window where no competitive experimental limit currently exists, making HIAF uniquely suited for this search.

HIAF

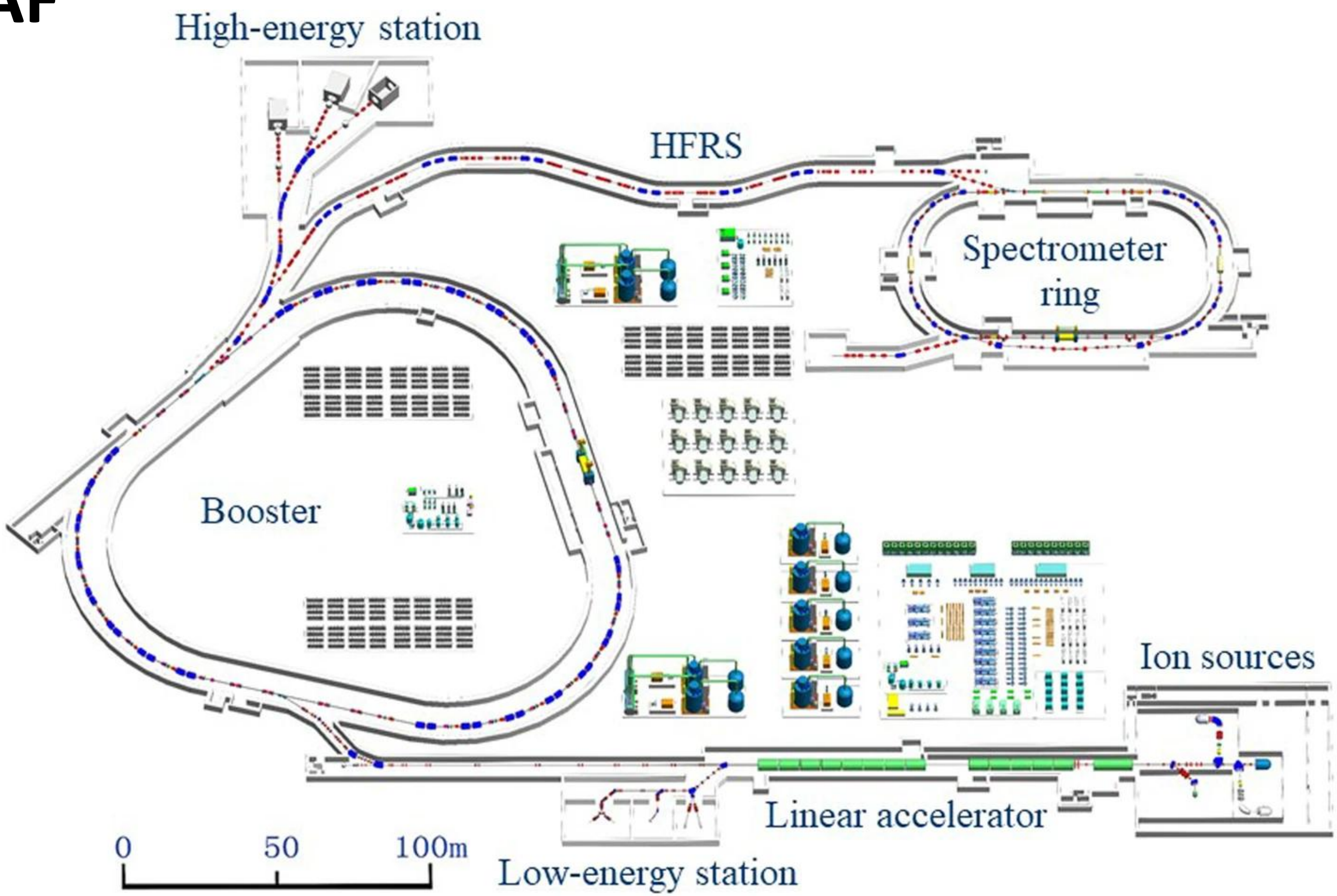

doi:10.1103/PhysRevAccelBeams.28.053401

HIAF

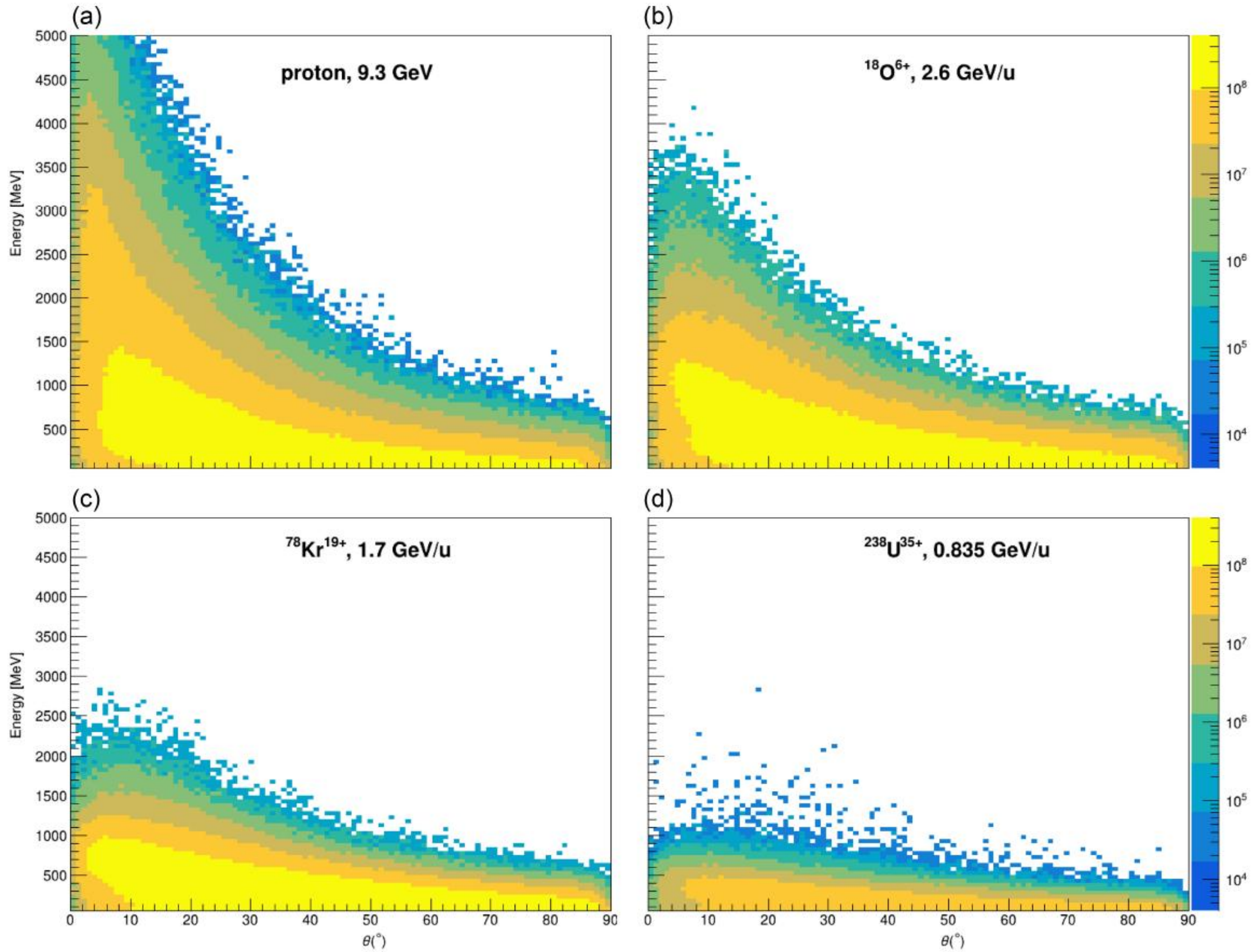

FIG. 2. Kinetic energy vs scatter angle distribution of π^+ generated after the production target with different bombarding beams, as shown in Table I. (a) Pion yield Y_{π^+} with proton beam, (b) pion yield Y_{π^+} with $^{18}O^{6+}$ beam, (c) pion yield Y_{π^+} with $^{78}Kr^{19+}$ beam, (d) pion yield Y_{π^+} with $^{238}U^{35+}$ beam.

DREAMuS

DREAMuS: Dark matter REsearch with Advanced Muon Source

Xiang Chen,[1,2,3] Zejia Lu,[1,2,3] Liangwen Chen,[4,5,6] Jun Gao,[1,2,3] Shao-Feng Ge,[7,2,3] Zhanxu Hao,[1,2,3] Yang Hu,[1,2,3] Bingzhi Li,[8] Cen Mo,[1,2,3] Zhiyu Sun,[4,5,6] Huayang Wang,[1,2,3] Chonghao Wu,[1,2,3] Yu Xu,[4,5] Xueheng Zhang,[4,5,6] Yulei Zhang,[9,a] and Liang Li[1,2,3,*]

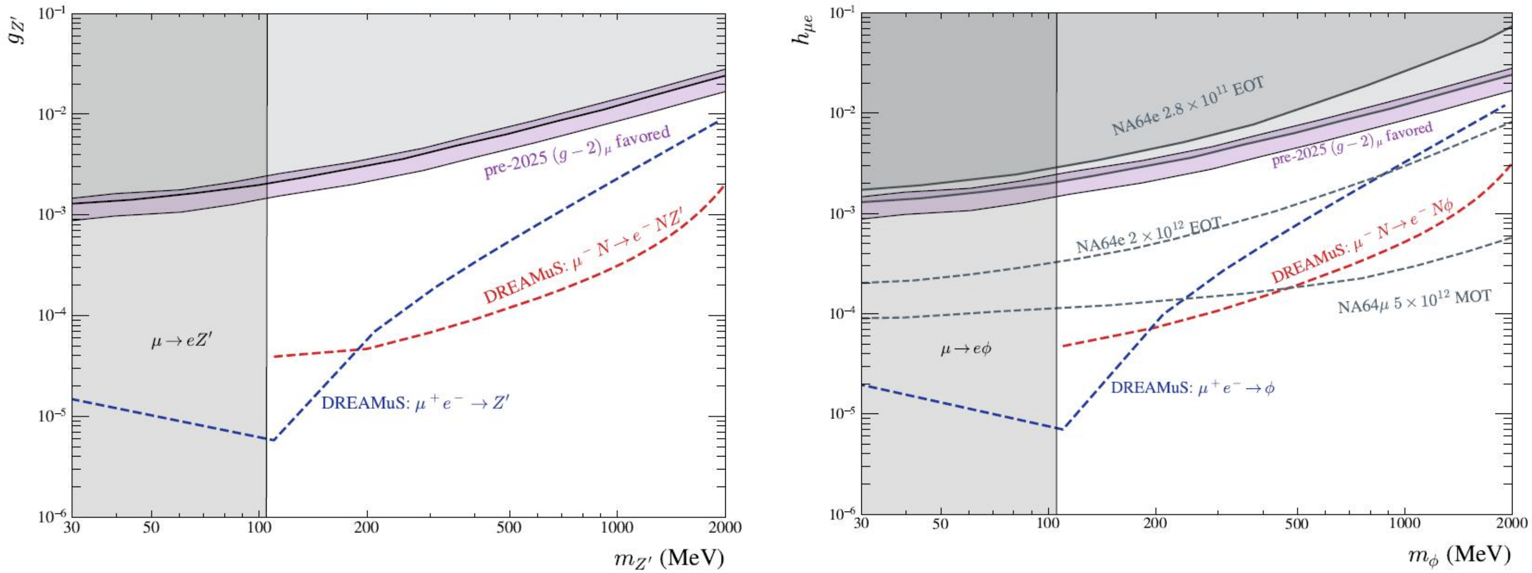

FIG. 7. Projected DREAMuS sensitivity to flavor-violating mediator couplings at the 90% C.L.. The left panel shows the expected reach for the vector mediator coupling $g_{Z'}$ as a function of the mediator mass $m_{Z'}$, while the right panel shows the corresponding reach for the scalar mediator coupling $h_{\mu e}$ in the ϕ scenario. In both panels, the red dashed curves correspond to the radiation channel and the blue dashed curves to the annihilation channel. The shaded regions are excluded by existing constraints [34], and the purple band indicates the parameter space favored by the pre-2025 $(g-2)_\mu$ anomaly [8, 10, 11]. The projected sensitivities of NA64$_e$ and NA64$_\mu$ are taken from Refs. [18, 33].